High-Precision Control for Ball-Screw-Driven Stage in Zero-Speed Region by Explicitly Considering Elastic Deformation

Hongzhong Zhu, Hiroshi Fujimoto (The University of Tokyo)

Abstract

Ball-screw-driven stages are extensively used in industry for high-precision fabrication thanks to the low cost and high efficiency. However, spring-like nonlinear friction in zero-speed crossing region significantly affects the control performance. In this paper, the mechanical deformation patterns at zero-speed point after slow deceleration and after fast deceleration are analyzed. It is shown that friction compensation methods in zero-speed region should take the elastic deformation patterns into account. Then, a new variable is defined to evaluate the variations of elastic deformation in the mechanical components. Finally, a novel friction compensation method for fast reverse motion using Sigmoid function is proposed to enhance the control performance by explicitly considering the elastic deformation, and the effectiveness is verified by experiments.

Key words: ball-screw-driven stage, friction compensation, elastic deformation, Sigmoid function

1. Introduction

Ball screws are linear actuators that can translate rotational motion to linear motion with little friction and high efficiency, and are extensively used in industrial applications. As the fast and precise positioning/servo control is increasingly required to improve the productivity, controllers with higher robustness become necessary [1]–[3]. However, due to the nonlinearity of the rolling friction which originates at elastic deformation of the mechanical components, the control performance would be significantly degraded at low speed motion, especially in the zero-speed crossing region where the so-called quadrant glitch phenomenon [4] [5].

Regard the nonlinear friction as a sort of disturbance, a well-known method for suppressing friction effects is the method referred to as disturbance observer (DOB) [6] [7]. This method can theoretically nominalize the control plant so that the control performance can be significantly improved [5]. However, due to the phase lag of the introduced low-pass filter and the inaccuracy of velocity signal at low-speed motion, the effects caused by nonlinear friction at zero velocity cannot be completely suppressed. Because of this reason, disturbance observer method and friction compensator coexist in many proposed approaches [3].

Another line for suppressing friction effects is to obtain precise friction model. For instance, Dahl model as well as LuGre model is proposed to explain the spring-like behavior in stiction [8] [9]. Swevers *et al.* also presented a complete and accurate model that can describe the hysteresis characteristics of the friction [10]. Based on the friction models, accurate friction compensation can be applied via feedforward/feedback manners. However, the models are so complex that not only the identification of the parameters but also the implementation to real systems are not easy problems. In order to take more priority over the ease of implementation, a heuristic friction model, which is also referred to as the Generalized Maxwell-Slip Model (GMS), was pro-

posed in [11]. However, the identification for the model is also a time-consuming task. Furthermore, it should be noticed that most of the proposed approaches only considered the compensation of velocity reversal motion, which may not enough for complex machining. For instance, if the stage is decelerated to zero velocity and then accelerated in the same direction, the elastic deformation in mechanical components would be different with reversal motion [12].

For tracking control, not only the precise mathematical model of the nonlinear friction is necessary, a proper compensation strategy is also required. The research in the literature considered to compensate the friction from the zero-speed point [13] [14]. However, the mechanical elastic deformation patterns at the point are not taken into account. In practical situations, the deformation patterns would greatly degrade the compensation performance even when the friction model is precise. Motivated by this perspective, we firstly study the elastic deformation patterns at the zero-speed point. It is pointed out that the conventional compensation methods are suitable for only slow reverse/non-reverse motions. For the case of fast reverse/non-reverse motions, some other compensation strategy becomes necessary.

The remainder of this study is organized as follows. Section II described the experimental setup and problem description. Section III analyzes the deformation characteristics of ball-screw stage in the zero-speed region. A friction compensation approach based on Sigmoid function for the fast reverse motion is proposed in Section IV. Experiments are performed to show the applicability of the proposed approach in Section V. The conclusion is summarized in Section VI.

2. Experimental setup and problem description

2.1 Experimental setup Fig. 1(a) shows the overview of the experimental X–Y ball-screw stage. The structure is shown in Fig. 1(b). Here, x_t denotes the po-

(a) Experimental device.
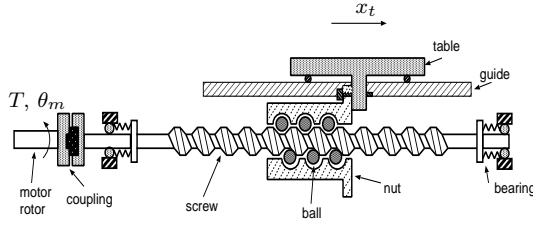
(b) Structure.

Fig. 1. Ball screw driven stage.

Table 1. Parameters of the stage in X-axis direction

motor inertia moment J_m	2.3×10^{-3} kgm^2
motor viscosity coefficient B_m	1.1772 Nms/rad
length of ball screw L_b	1.169 m
mass of ball screw M_b	9.3526 kg
inertia moment of ball screw J_b	1.0052×10^{-3} kgm^2
viscosity coefficient of ball screw B_b	5.0×10^{-2} Nms/rad
lead of ball screw L_p	1.2×10^{-2} m
mass of table M_t	273.0 kg
viscosity coefficient of linear guide C_t	1.0×10^4 Ns/m

sition of the stage, θ_m denotes the rotation angular of the motor, and T denotes the motor torque. Table. 1 shows the parameters of the stage in X-axis direction. Ball screw is directly connected with the shaft of servo motor through the coupling. The servo motor is equipped with an absolute encoder whose resolution is 2^{20} pulses/rev. A linear scale with a resolution of 100nm is applied to measure position information of the stage.

The rigid-body model of the stage is expressed as follows:

$$ P_n(s) := \frac{K_\tau}{Js^2 + Bs}, \dots\dots\dots\dots\dots\dots\dots\dots \text{(1)} $$

where $K_\tau = 0.715$ Nm/A is the torque constant, J is the nominal inertia and B is the nominal viscosity. According to an identification experiment, the parameters in (1) is assigned as $J = 0.01$ kgm^2 and $B = 0.1$ Nms/rad. Fig. 2 shows the frequency response of the experimental device, and the fitted model is shown by the solid line.

2.2 Controller design The block diagram of con-
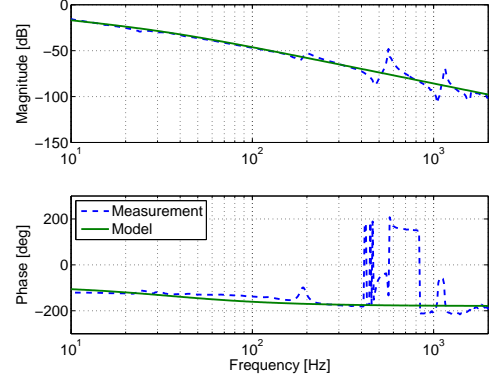
Fig. 2. Frequency response of stage from the current input to motor position θ.
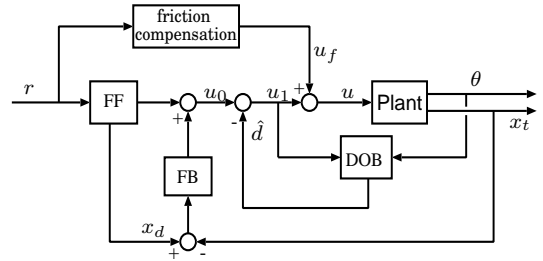
Fig. 3. Block diagram of control system with two-degree-of-freedom controller, an inverse-model-based disturbance observer and feedforward friction compensation.
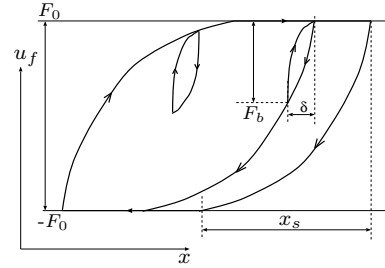
Fig. 4. Rolling friction model.

trol system is shown in Fig. 3. r is the trajectory reference, and u is the control input. The feedforward controller is designed as the stable inverse system of the nominal plant via Perfect tracking control (PTC) [15]. The perfect tracking at every sampling instant can be theoretically guaranteed. x_d is the desired reference. A PID compensator, designed by pole assignment approach, is applied as the feedback controller. The resulting bandwidth of the closed loop is 20 Hz. Friction compensation is also considered, which will be studied in the following. u_f is the friction compensation signal. Additionally, an inverse-model-based disturbance observer (DOB) is designed using the motor velocity information [6]. A 1$^\text{st}$-order low-pass filter is designed for the disturbance observer with the bandwidth of 80 Hz. A high-performance DSP(TMS320C6713, 225MHz) is used as the processor to implement the controller. $\hat{d}$ is the estimated disturbance. The PID compensator, DOB and friction compensation are discretized by 0.5 ms, and the sampling period for PTC is 1 ms.

2.3 Problem description Conventional friction
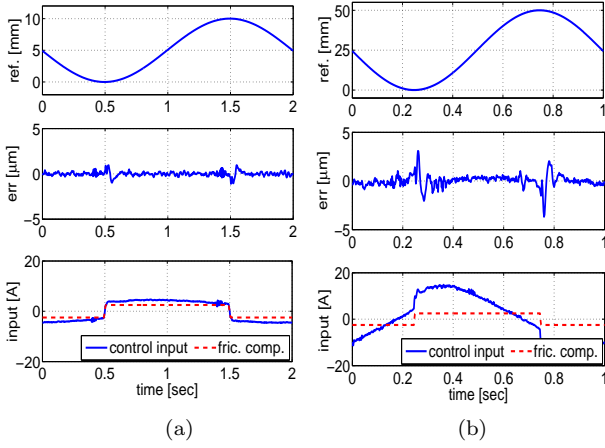
Fig. 5. Experimental results of a slow reverse motion (a) and a fast reverse motion (b). The upper graphs show the trajectory references; The middle graphs show the tracking errors; And the lower graphs show the control input and compensated friction.
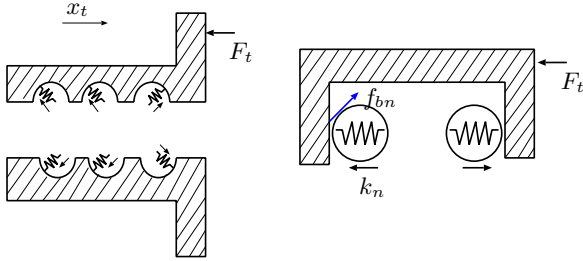
Fig. 6. Force analysis of the nut and the model.

compensation methods treat the friction as a springlike friction having the hysteresis characteristics shown in Fig. 4. Here, x_s denotes the pre-sliding regime and F_0 is the Coulomb friction. Based on some sophisticated friction model, these methods compensate the friction from the zero-speed point without considering the initial state of the elastic deformation. In practical situation, initial deformation of mechanical components plays a dominant role in the performance degradation. It will be illustrated that the elastic deformation pattern after slow deceleration is different with the pattern after fast deceleration. It is the difference that makes the conventional compensation approach do not work well in fast reverse motion, as shown in Fig. 5. In both experiments, friction compensation was performed from the reverse points using rolling friction model Fig. 13. It is observed that the compensation performance is remarkably degraded in fast reverse motion. In the next section, the elastic deformation characteristics in zero-speed region is studied in detail.

3. Deformation characteristics in zero-speed region

3.1 Dynamics of ball-screw stage Suppose that the balls between nut and screw are small and weightless, we can treat the balls as nonlinear springs. The force analysis of the nut and the model are shown in Fig. 6. Here, the forces in z-axis direction is ignored since they are balanced. F_t denotes the counteracting force from the table, and f_{bn}
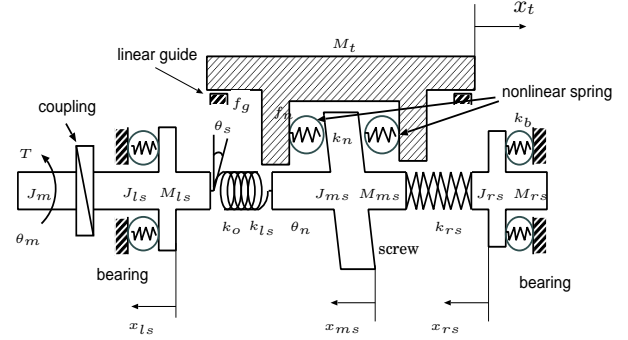
Fig. 7. Mechanical model of the ball screw drive system.

denotes the friction between the ball and nut.

Based on the nut model, the ball-screw-driven stage can be modelled as Fig. 7 if the stiffness between the nut and the table is rigid enough. Here, the screw is divided into three parts, and the inertia/mass of each part is denoted as J_{xs}/M_{xs}, where the subscript x is l (left part), m (middle part) or r (right part). k_o is the torsional stiffness of the screw from the motor to the nut, k_{ls} and k_{rs} are the axial stiffness, k_b is the stiffness of bearings, k_n is the stiffness of screw-ball-nut, f_g is the friction of the guide way, f_n is the friction between nut and ball, and θ_s is the rotational displacement of the screw. In the following, we analyze the elastic deformation starting from the force analysis of the table.

3.2 Deformation patterns in zero-speed region The motion equation of the table can be expressed by

$$M_t \ddot{x}_t = F_{bn} - f_g, \cdots\cdots\cdots\cdots\cdots\cdots\cdots\cdots\cdots (2)$$

where f_g is the friction from the linear guide. F_{bn} is the drive force from the screw to the nut&table in the moving direction via the rolling balls. For the ease of analysis, the elastic deformation of the screw-ball-nut at zero-speed point after slow deceleration and fast deceleration is taken into account. In the case of slow deceleration, the left side of (2) is small so that the force F_{bn} is applied for overcoming the friction f_g. In the process, the force F_t (counteracting force of F_{bn}) need to be balanced by the supporting force of the bearings at the left side of the screw. Therefore, the deformation characteristics of the screw-ball-nut at zero-speed point can be illustrated in Fig. 8. In the figure, right side of the grooves in the nut, left part of the screw, and the bearings at the left side of the screw are compressed. During this deceleration, the drive force F_{bn} does not change its direction. This can be confirmed by experimental result shown in Fig. 5(a). For convenience, the deformation of this kind is denoted as *Pattern I*. On the other hand, in the case of fast deceleration, the left side of (2) is larger than the friction so that the external force F_{bn} is applied to break the motion before the velocity come to zero. Therefore, F_{bn} changed its direction before the velocity comes to zero-speed point, as shown in Fig. 5(b). The deformation characteristics is illustrated in Fig. 9. In this case, left side of the grooves in the nut, right part of the screw, and the bearings at the right side are compressed. The elastic deformation of this kind is denoted as *Pattern II*. Therefore, it is obtained that the elastic deformation of screw-ball-nut at zero-speed point has two patterns. In ad-
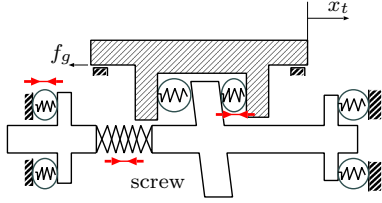
Fig. 8. Elastic deformation after slow deceleration. Right side of the grooves in the nut, left part of the screw, and the bearings at the left side of the screw are compressed. This pattern is denoted as *Pattern I*.
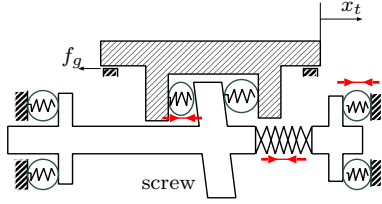
Fig. 9. Elastic deformation after fast deceleration. Left side of the grooves in the nut, right part of the screw, and the bearings at the right side are compressed. This pattern is denoted as *Pattern II*.

dition, the elastic deformation of mechanical components is not changed during the slow deceleration. However, in the case of fast deceleration, the deformation pattern is changed before the velocity comes to zero. In the following, we will analyze how the patterns affect the control performance in the coming acceleration motion.

Firstly, the reverse motion is considered. The drive force F_{bn} is applied to overcome the friction f_g and drive the table in the reverse direction. Therefore, Left side of the grooves in the nut and the bearings at the right side of screw will be compressed to generate the drive force, which is actually the pattern shown in Fig. 9. Therefore, in the case of slow reverse motion, the elastic deformation should be shifted from *Pattern I* to *Pattern II*. This is the case considered by conventional methods which compensate the friction from the reverse point following the hysteresis curve shown in Fig. 4. On the other hand, in the case of fast reverse motion, the elastic deformation is from *Pattern II* to *Pattern II*, which is different from the case of slow reverse motion. Therefore, the conventional methods will not compensate the friction perfectly.

Then, we analyze the case of non-reversal motion where the coming acceleration motion will be in the same direction with the deceleration. In this case, the force F_{bn} is also in the acceleration direction. Therefore, the deformation state after the zero-speed point is shown in Fig. 8. When this motion is after a slow deceleration, the elastic deformation is from *Pattern I* to *Pattern I*. A sinc-function-based friction compensation method developed by our group is verified to be effective for this case [12]. However, when the coming motion is after a fast deceleration, the elastic deformation should be shift from *Pattern II* to *Pattern I*. In this case, F_{bn} will change its direction drastically and a rebound phenomenon may also be caused.

3.3 Validation of deformation In order to validate the deformation of elastic components, a variable is
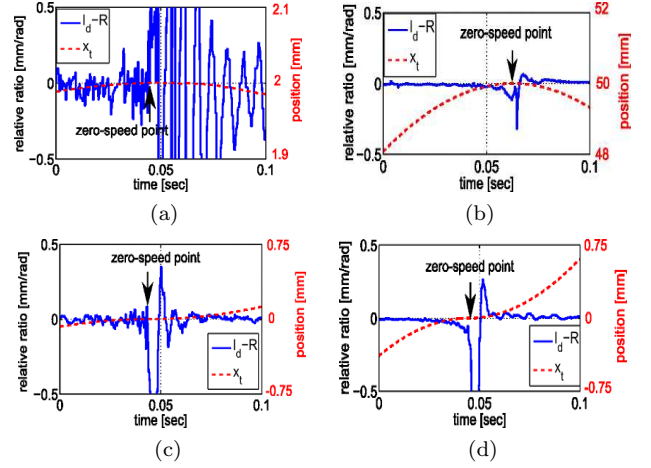
Fig. 10. Comparison of the relative ratio $l_d - R$ and the stage position of four cases. (a): Slow reverse motion; (b): Fast reverse motion; (c): slow non-reverse motion; (d): fast non-reverse motion.

defined as follows:

$$l_d := \frac{\frac{d\,x_t}{d\,t}}{\frac{d\,\theta_m}{d\,t}} = \frac{d\,x_t}{d\,\theta_m}. \cdots\cdots\cdots\cdots\cdots\cdots\cdots\cdots\cdots (3)$$

In discrete-time realization, the approximation that

$$l_d = \frac{d\,x_t}{d\,\theta_m} \approx \frac{\Delta x_t}{\Delta \theta_m} \cdots\cdots\cdots\cdots\cdots\cdots\cdots\cdots\cdots (4)$$

are applied. Here, Δx_t and $\Delta \theta_m$ are the position/angular displacement in a given short period T_p. In the ideal case without any elastic deformation, The value of l_d is the same with the rotation-to-translation ratio R of the screw. However, due to the dynamic deformation of the mechanical components, l_d varies when the drive force or cutting force fluctuates, especially in the zero-speed crossing region. Experimental results of four cases of slow reverse motion, fast reverse motion, slow non-reverse motion and fast non-reverse motion are shown in Fig. 10. In the cases of fast motion, l_d gradually reduced before the velocity comes to zero. On the other hand, in the cases of slow motion, though l_d cannot be calculated correctly due to the effects of position measurement error, it can be observed that the nominal value of l_d remains constant before the velocity comes to zero. Therefore, the analysis in last subsection is verified.

For precise tracking control, the initial deformation states are required to be taken into account on friction compensation. In the following section, a novel compensation method is proposed for the case of fast reverse motion. The summary of friction compensation for ball-screw-driven stage is indicated in Table. 2.

4. Sigmoid-function-based friction compensation for fast reverse motion

There is much research focusing on torque compensation in reversal motions, and it is widely known that the dynamics has hysteresis phenomenon shown in Fig. 4. The friction model of this case is usually obtained by applying some small

Table 2. Summary of friction compensation in zero-speed region

Type of motion	Elastic deformation	Compensation method
slow reverse	Pattern I → Pattern II	compensation after zero-speed point [8] [11] [3] [13] [14] etc...
fast reverse	Pattern II → Pattern II	compensation before zero-speed point (proposal of this study)
slow non-reverse	Pattern I → Pattern I	compensation after zero-speed point [12]
fast non-reverse	Pattern II → Pattern I	redesign of trajectory reference is necessary
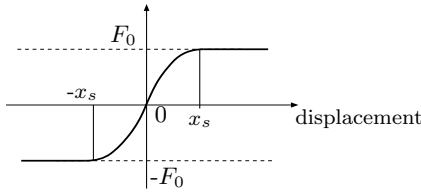
Fig. 11. Sigmoid function applied for nonlinear friction compensation.

Fig. 12. Rolling friction characteristic.

Fig. 13. Comparison of the real rolling friction and sinc function based model.

and low frequency sinusoidal reference signal to the control system and analyzing the relationship between applied input and the controlled output. In the case of slow reverse motion, the motion condition is the same with this model identification condition. Therefore, the conventional compensation methods can work well. In the case of fast reverse motion, motion condition is very different with model identification condition. Therefore, the friction compensation for fast reverse motion is required to be further studied.

As shown in Fig. 10(b), l_d decreases during the deceleration before the stage comes to stop. The applied input is used for "breaking" the stage. Due to the elastic deformation, the overrun of the stage may happen in this process. In order to cope with the problem, a compensation method consists of breaking the stage before it comes to stop and overcome the nonlinear friction after the reverse is considered.

The compensation method based on Sigmoid function is determined by

$$u_f = F_0 \frac{x/\sigma}{\sqrt{1 + (x/\sigma)^2}}, \quad\quad\quad\quad\quad\quad (5)$$

where x is the displacement from the reversal point, and σ is a parameter related to the spring-like pre-sliding regime that should be identified. The compensation idea is shown in Fig. 11. Consider the case of fast reverse motion where the velocity is from positive direction to negative direction, the drive force F_{bn} is applied to brake the motion before the stage comes to stop. In this case, the friction compensation u_f is reduced from F_0 to 0 to help brake the motion. In the acceleration process, u_f is increased from 0 to F_0 to compensate the friction. A similar analysis can be obtained when the velocity is from negative direction to positive direction.

In next section, experiments will be performed to shown the effectiveness of this proposal method.
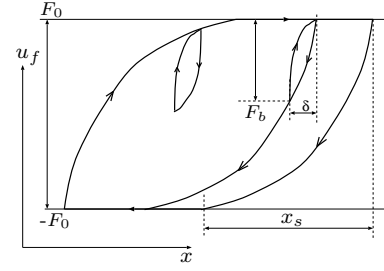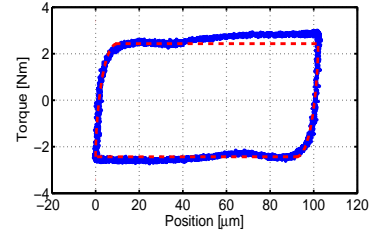
5. Experiments

A sine signal $x_t^*(t) = 25(1 - \cos(2\pi t))$mm whose maximum deceleration is $100\pi^2$mm/s^2 is applied as the trajectory reference to evaluate the friction compensation performance. For the experimental device shown in Section 2, this trajectory in the zero-speed region can be regarded as fast reverse motion. For comparison, two conventional compensation methods are introduced.

5.1 Sinc-function-based friction compensation [12]
Sinc function applied to fit the rolling friction is expressed by

$$u_{f_a} = \begin{cases} -F_0, & x < 0 \\ 2F_0 \dfrac{\sin\left(\pi\sqrt{\frac{x}{x_s}} - \pi\right)}{\pi\sqrt{\frac{x}{x_s}} - \pi} - F_0, & 0 \le x < x_s \\ F_0, & x \ge x_s \end{cases} \quad \cdot (6)$$

where x is the displacement of position from the zero-speed point of the case the velocity is changed from negative direction to positive direction, x_s is the length of the presliding regime, and F_0 can be regarded as the Coulomb friction. In [12], this method is applied for the slowly reversal motion and the effectiveness has already been verified by experiments. The comparison of the real rolling friction and the sinc-function-based model is shown in Fig. Fig. 13, where $x_s = 10\,\mu$m and $F_0 = 2.431$ Nm.

5.2 Coulomb friction compensation In the case of fast reverse motion, it is analyzed in last section that elastic deformation patterns before and after the reverse point are the same. Therefore, the dynamics of deformation during the reverse may be considered to be ignored. Based on this analysis, it is reasonable to only consider the compensation for Coulomb friction. The following compensation strategy is considered.

$$u_{f_a}(d) = \begin{cases} F_0, & \text{v} < 0 \\ -F_0, & \text{v} \ge 0 \end{cases}, \quad\quad\quad\quad\quad\quad (7)$$
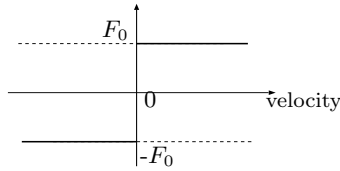
Fig. 14. Friction compensation based on Coulomb friction model.
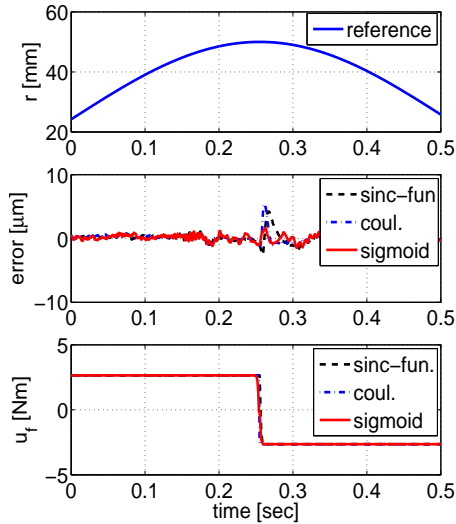
Fig. 15. Experimental results.

Table 3. Comparison of friction compensation effects

	Sinc-function	Coulomb friction	Sigmoid function
Maximum error $[\mu m]$	4.24	5.44	1.65

where F_0 can be regarded as the Coulomb friction. The compensation strategy is shown in Fig. 14.

5.3 Experimental results Coulomb friction F_0 of all three methods is set as $F_0 = 2.65\,\mathrm{Nm}$ based on the experimental result shown in Fig. 13. The parameters σ and x_s in (5) is set as $\sigma = 2$ and $x_s = 10\,\mu m$, respectively. The experimental results are shown in Fig. 15. The maximum error during the reverse motion is summarized in Table 3. It is observed that the Sigmoid-function-based compensation method obtains the best position tracking performance, and can reduce the tracking error before the reversal.

6. Conclusion

In this study, the elastic deformation of mechanical components of experimental ball-screw-driven stage is analyzed in detail. It is obtained that the elastic deformation patterns at zero-speed point are different between the cases after slow deceleration and the cases after fast deceleration. In addition, a new variable is defined in order to evaluate the dynamical deformation in the zero-speed region. Based on the deformation patterns, a novel nonlinear compensation method based on Sigmoid function is proposed for fast reverse motion.

References

(1) F. Huo, and A.-N. Poo, "Precision Contouring Control of Machine Tools", *Int. J. Adv. Manuf. Technol.*, Vol. 64, pp. 319–333, 2013.

(2) M. Iwasaki, K. Seki, and Y. Maeda, High-Precision Motion Control Techniques–A Promising Approach to Improving Motion Performance, *IEEE Trans. Ind. Electron. Magazine*, Vol. 6, No. 1, pp.32-40, 2012.

(3) Z. Jamaludin, H. V. Brussel, and J. Swevers, Friction Compensation of an XY Feed Table Using Friction-Model-Based Feedforward and an Inverse-Model-Based Disturbance Observer, *IEEE Trans. Ind. Electron.* , Vol. 56, No. 10, 2009.

(4) M. Iwasaki, M. Miyaji, N. Matsui, High-Precision Contouring Control of Table Drive System in Machine Tools Using Lost Motion Compensation, *IEEJ Trans. IA*, Vol. 125, No. 6, pp.616-622, 2005.

(5) H. S. Lee and M. Tomizuka, Robust Motion Controller Design for High-Accuracy Positioning Systems, *IEEE Trans. Indust. Electr.* , Vol. 43, No. 1, pp. 48–55, Feb. 1996.

(6) T. Umeno and Y. Hori, Robust Speed Control of DC Servomotors Using Modern Two Degree-of-Freedom Control Design, *IEEE Trans. Indust. Electr.* , Vol. 38, No. 5, pp. 363–368, Oct. 1991.

(7) S. Sakai and Y. Hori, Ultra-low Speed Control of Servomotor using Low Resolution Rotary Encoder, in *Proc. IECON 21st int. Conf. Ind. Electron.* , Orlando, FL, Vol. 1, pp. 615–620, 1995.

(8) C. Canudas de Wit, H. Olsson, K. Astrom and P. Lischinsky, A new model for control of systems with friction, *IEEE Trans. Autom. Control*, Vol. 40, No. 5, pp. 419-425, 1995.

(9) P. Dahl, A solid friction model, Aerospace Corp., El Segundo, CA, Tech. Rep. TOR-0158(3107-18), 1968.

(10) J. Swevers, F. Al-Bender, C. G. Ganseman, and T. Prajogo, An integrated friction model structure with improved presliding behavior for accurate friction compensation, *IEEE Trans. Automat. Contr.*, Vol. 45, pp. 675–686, Apr. 2000.

(11) F. Al-Bender, V. Lampaert and J. Swevers, The Generalized Maxwell-Slip Model: A Novel Model for Friction Simulation and Compensation, *IEEE Trans. Autom. Control*, Vol. 50, No. 11, pp. 1883-1887, 2005.

(12) H. Zhu and H. Fujimoto, Proposal of Nonlinear Friction Compensation Approach for a Ball-Screw-Driven Stage in Zero-Speed Region including Non-Velocity-Reversal Motion, *IECON 2013*, to be presented.

(13) C.L. Chen, M.J. Jang, and K.C. Lin, "Modeling and High-Precision Control of a Ball-Screw-Driven Stage", *Precision Engineering*, Vol. 28, pp. 483–495, 2004.

(14) Y. Maeda, and M. Iwasaki, "Analytical Examinations and Compensation for Slow Settling Response in Precise Positioning Based on Rolling Friction Model", *Advanced Motion control* , pp. 24–29, Nagaoka, Mar. 2010.

(15) H. Fujimoto, Y. Hori, and A. Kawamura, Perfect Tracking Control based on Multirate Feedforward Control with Generalized Sampling Periods, *IEEE Trans. Ind. Electron.*, Vol. 48, No. 3, pp.636-644, 2001.